The Effect of Antecedent Topography on Complex Crater Formation

Don R Hood¹, Brennan Young², Aviv Lee Cohen-Zada², Peter Benjamin James¹, Ryan C. Ewing², and Jeffery S. Lee³

¹Baylor University ²Texas A&M University ³Baylor University

March 07, 2024

Abstract

Impact craters that form on every planetary body provide a record of planetary surface evolution. On heavily-cratered surfaces, new craters that form often overlap older craters, but it is unknown how the presence of older craters alters impact crater formation. We use overlapping complex crater pairs on the lunar surface to constrain this process and find that crater rims are systematically lower where they intersect antecedent crater basins. However, the rim morphology of the new crater depends on both the depth of the antecedent crater and the degree of overlap between the two craters. Our observations suggest that transient rim collapse is altered by antecedent topography, leading to circumferential distribution of rim materials in the younger crater. This study represents the first formalization of the influence of antecedent topography on rim morphology and provides process insight into a common impact scenario relevant to the geology of potential Artemis landing sites.

Hosted file

LunarCraterOverlapManuscript_GRL_V1.docx available at https://authorea.com/users/527609/ articles/714871-the-effect-of-antecedent-topography-on-complex-crater-formation

Hosted file

SupportingInformation.docx available at https://authorea.com/users/527609/articles/714871-the-effect-of-antecedent-topography-on-complex-crater-formation

1 The Effect of Antecedent Topography on Complex Crater

2 Formation

- 3 Don R. $Hood^1$
- 4 Brennan W. Young²
- 5 Aviv L. Cohen-Zada²
- 6 Peter B. James¹
- 7 Ryan C. $Ewing^2$
- 8 Jeffery S. Lee¹
- 9
- 10 $\frac{1}{2}$ Baylor University, Department of Geoscience
- 11 ² Texas A&M University Geology and Geophysics
- 12
- 13 Corresponding Author: Donald R Hood (<u>drhood2938@gmail.com</u>)
- 14
- 15 <u>Key Points</u>
- Overlapping complex crater rims are lower inside the antecedent basins compared to outside.
- Deeper antecedent basins and more significant crater overlap tend to create larger differences in rim height.
 - Changes in the impact crater formation process, mainly during transient rim collapse, influence the shape of overlapping crater rims.
- 21 22

23 <u>Abstract</u>

- 24 Impact craters that form on every planetary body provide a record of planetary surface evolution.
- 25 On heavily-cratered surfaces, new craters that form often overlap older craters, but it is unknown
- 26 how the presence of older craters alters impact crater formation. We use overlapping complex
- 27 crater pairs on the lunar surface to constrain this process and find that crater rims are
- 28 systematically lower where they intersect antecedent crater basins. However, the rim
- 29 morphology of the new crater depends on both the depth of the antecedent crater and the degree
- 30 of overlap between the two craters. Our observations suggest that transient rim collapse is altered
- 31 by antecedent topography, leading to circumferential distribution of rim materials in the younger
- 32 crater. This study represents the first formalization of the influence of antecedent topography on
- rim morphology and provides process insight into a common impact scenario relevant to the
- 34 geology of potential Artemis landing sites.
- 35

36 <u>Plain Language Summary</u>

- 37 Craters form on the surface of every planetary body and help us to understand many qualities of
- the surface including, critically, the age of the surface. On older surfaces with many craters, new
- craters that form often overlap and partially destroy older craters, though we don't know if or
- 40 how the presence of the older crater changes the processes that create the new crater. Looking at
- 41 large Lunar craters, we can determine that the presence of an older crater causes the rim of the
- 42 new crater to be asymmetric: lower where it forms within the older crater basin. The difference
- 43 in height between the new crater rim inside and outside the old crater depends on both the depth
- 44 of the older crater, and where the new crater forms relative to the older crater. From this we can
- 45 interpret that the presence of the older crater alters the way the new crater forms, leading to an
- 46 uneven collapse of early rim materials.
- 47

48 <u>1. Introduction</u>

49 Impact cratering sculpts the topography of all solid planetary bodies and is singularly important on airless bodies like the Moon. The genesis of crater morphology, its evolution, and relationship 50 51 to the impact process is the subject of numerous experiments (Aschauer and Kenkmann, 2017), 52 models (Elbeshausen et al., 2009; Krohn et al., 2014; Wünnemann and Ivanov, 2003), and 53 surveys (Robbins, 2019; Wang et al., 2021). These studies establish clear relationships between 54 crater morphology and impact process, enabling investigations of planetary regolith (Izquierdo et 55 al., 2021), buried ice (Bramson et al., 2015; Dundas et al., 2021), and surface age (Hartmann and 56 Neukum, 2001) based on crater morphology and physical properties. However, impact crater models generally disregard the influence of antecedent topography in the target on the final 57 58 crater shape. Studies of simple craters in high-relief terrains (Aschauer and Kenkmann, 2017; 59 Krohn et al., 2014) demonstrate that antecedent slopes influence crater morphology, but it is 60 frequently assumed that complex craters obliterate the underlying topography (Hirabayashi et al., 2017; Riedel et al., 2020). Martian craters that straddle the topographic dichotomy, such as Gale 61 62 Crater (Schwenzer et al., 2012) and Gusev Crater (Parker et al., 2010), have lower northern rims, 63 possibly due to the influence of the topographic dichotomy. Additionally, prior observational investigations of lunar craters have found that low points in the crater rim are frequently aligned 64 65 with downslope directions in local topography rather than downrange impact direction (Neish et al., 2017, 2014).

66 67

68 It is clear from these studies that antecedent topography influences the crater formation process

and potentially the morphology of the impact crater, but these effects are largely unquantified

and do not address a common type of antecedent topography: the presence of an older crater.

71 This represents a gap in knowledge about the connection between crater morphology and impact

72 processes, limiting our use of craters as an exploratory tool to probe planetary surfaces. Here, we

examine many overlapping, complex lunar craters (Figs. 1, 2) to quantify the influence of

antecedent topography on crater morphology. Specifically, we test the hypothesis that crater rims

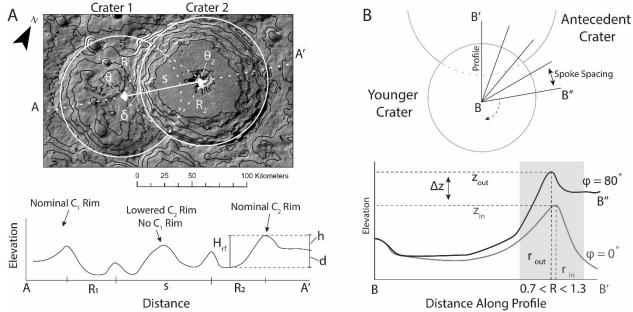
exhibit lower elevations where they overlap antecedent crater basins compared to where they do

not. We do so by systematically examining overlapping crater pairs on the lunar surface and
 determining if crater rims forming in antecedent crater basins are systematically lower relative to

determining if crater rims forming in antecedent crater basins are systematically lower relative tothe rim that falls outside the antecedent crater. Furthermore, we characterize the magnitude of

78 the finit tails outside the antecedent crater. Furthermore, we characterize the magnitude of 79 these differences and establish relationships between rim elevation differences, crater geometry,

80 and the degree of crater overlap.



82

83 Fig. 1. (A) An overlapping crater pair with 1 km topographic contours overlain on surface

84 *imagery (top) and a topographic profile through both craters' centers (bottom). (B) Crater*

- Analysis scheme in plan and profile view. In A, the larger crater (Crater 2) is the younger crater,
 and the smaller crater (Crater 1) is antecedent to Crater 2. The rim of Crater 2 is ~1 km lower
- where it overlaps Crater 1. See Supporting Information and Table S1 for mathematical
- 88 *notations*.
- 89

90 <u>2. Data & Methods</u>

91 2.1 Datasets & Crater Pair Selection

We use the Global Lunar DTM 100 (GLD100) for our topographic analysis as it has near-global
 coverage (79°S - 79°N) of the lunar surface at high spatial resolution (100 m) (Scholten et al.,

- 94 2012). Among the recent global datasets of lunar craters (Robbins, 2019; Wang et al., 2021), we
- use the Robbins, 2019 (Robbins, 2019) crater database because it represents a highly complete
- 96 catalog of lunar craters at least 2 km in diameter, and it provides important characterizations of
- 97 crater geometry that are necessary for our study. We evaluate only craters with ellipticities (ε)
- 98 less than 1.3 to avoid the additional complexities and asymmetries associated with oblique
- impacts and reduce the population of secondary impacts within our analysis (McEwen and
- Bierhaus, 2006). Our focus on highly circular craters allows us to reduce the complexity of our
- approach by using the best-fit circular diameter rather than elliptical geometry. We also limit our analysis to craters between 17 and 400 km in diameter (D) to analyze only craters within the
- 103 complex regime (Pike, 1977). We use the Wide Angle Camera morphology mosaic (Speyerer et
- al., 2011) for manual relative crater age assessment.
- 105

106 2.2 Determination of Crater Morphometry

- 107 For every overlapping crater pair, we extract topographic profiles oriented radially about each
- 108 crater's centroid. Using these profiles, we examine how crater-rim elevation (z) and distance
- 109 from the crater centroid (*r*) change azimuthally (Fig. 1). We perform a preliminary low-
- 110 resolution survey (profile point spacing of 400 m and a spoke spacing of 10°) on both members
- 111 of each crater pair to determine their relative ages. Then, we analyze the younger crater with a

point spacing of 100 m and spoke spacing of 5° to produce our final observations. We use a

definition of crater rim similar to a recent crater survey of craters on the moon (Wang et al.,

114 2021), selecting the rim to be the maximum-altitude location between 0.7 and 1.3R,

115 accommodating craters up to $\varepsilon = 1.3$.

116

117 2.3 Crater-Pair Observations

There are several morphometric parameters that we measure to determine which crater in each pair is younger as well as investigate the effects of antecedent topography. Specifically: (1) we measure the peak rim elevation (z) and rim location (r) along each topographic profile; (2) we measure the difference in crater rim elevation between the area inside (z_{in}) and outside (z_{out}) the intersection arc; (3) we measure the degree of overlap between the two craters; and (4) we predict the depth of the older crater relative to the undisturbed surface. We measure the height difference between the rim inside and outside the intersection arc as:

125 126

$$\Delta z = \bar{z}_{in} - \bar{z}_{out} \text{ , and} \tag{1}$$

$$\max(\Delta z) = \min(z_{in}) - \bar{z}_{out} . \tag{2}$$

128

129 To understand their general relationships, we normalize the difference in rim elevation (Δz or 130 $max(\Delta z)$) by the predicted depth of the older crater (d) based on scaling laws ($d=H_{rf}$ - h; Pike,

131 1977). Where $\Delta z/d = 0$, the rim of the younger crater is not lower where it overlaps the

antecedent topography compared to the rim outside this overlap. Negative values of $\Delta z/d$

133 generally indicate that the rim is lower where it overlaps antecedent topography, and a value of -

134 1 indicates that the rim is lowered by the expected depth of the pristine antecedent crater.

135

136 Complex craters are not perfectly cylindrical depressions; therefore, we expect that the $\Delta z/d$ of a crater pair will depend partially on where within the antecedent crater the younger crater rim 137 138 forms. We measure crater overlap using the distance between the antecedent crater center and the 139 younger crater rim (δ , Fig. 1) and normalize this distance to the older crater radius (R_a). To first 140 order, we expect $max(\Delta z)/d$ to decrease with increasing crater overlap, especially at lower 141 degrees of overlap. If $max(\Delta z)/d$ traces crater topography, it will decrease from near 0 to -1, 142 where the young crater rim forms in the antecedent crater floor. We expect that $\Delta z/d$ will be a 143 less-sensitive tracer of this pattern, as it averages across portions of the young rim that intersect 144 the antecedent rim and collapse terraces. We also examine profiles along rims intersecting

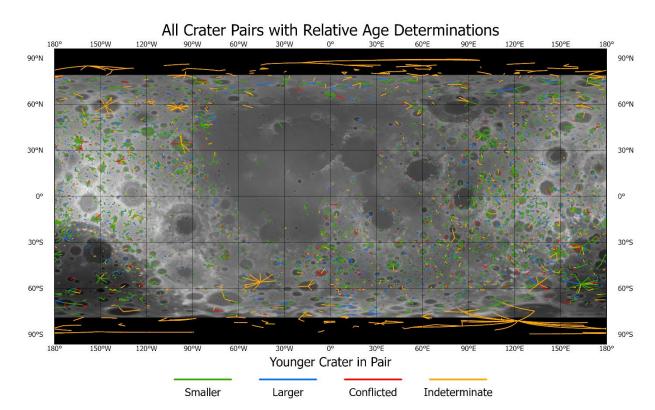
145 antecedent topography to determine how the new rim traces the expected antecedent topography 146 (Fig. 4). Rim elevation difference along individual profiles $((z - \bar{z}_{out})/d)$ is plotted as a

- function of azimuth normalized to the total intersection arc (φ') to enable averaging across
- 148 multiple crater pairs. We compare our observations of crater rim topography with the
- topography of Aristillus Crater (D = 53 km), a relatively pristine, complex crater located on the
- 150 Lunar nearside (Grier et al., 2001). We measure topography along the perimeter of three circular
- 151 "craters" (D = 35 km) that intersect Aristillus at distances of s = 21.5, 29.5, and 37.5 km,
- 152 corresponding to δ values of 0.15, 0.45, and 0.75 R_o , respectively. These measurements provide a
- proxy for the expected antecedent topography along a crater rim where it would intersect a
- prototypical complex crater. We normalize elevation along these profiles analogously to the individual nine mediate (-)
- individual rim profiles: $(z-z_{mare})/(z_{mare}-z_{floor})$ using the local mare elevation (z_{mare}) and crater floor elevation (z_{floor}) instead of the exterior rim and predicted crater depth. These comparisons
- demonstrate how the post-impact rim topography compares to the antecedent topography, how

- 158 much of the young rim forms within the antecedent crater floor, and whether the sharp,
- 159 antecedent terrace-to-floor transition is preserved in the young crater rim.
- 160

3. Results & Discussion 161

162



163

Fig. 2. Overlapping complex crater pairs after filtering and determination of relative age. Lines 164

- 165 connect the centers of each crater in the pair with color designating whether the relative age of craters in the pair was determined. Black areas near the poles indicate areas outside the
- 166
- coverage of the topographic dataset (Scholten et al., 2012). 167
- 168
- 169 3.1 Crater Pair Determination

170 Of the ~1.3 million craters in the crater database (Robbins, 2019), 8,653 meet our selection 171 criteria ($\varepsilon < 1.3$, 17 km < D < 400 km), from which we identified 4,932 craters that make 4,024 172 intersecting crater pairs (Fig. 2). These are predominantly found in the highlands due to the overall higher abundance of large (D > 17 km) craters. The smaller crater is determined to be 173 younger in 2,482 pairs (61.7%), and the larger crater is determined to be younger in 522 pairs 174 (12.9%). The relative ages of 1,020 (25.3%) pairs could not be determined, of which 393 (9.8%) 175 176 are caused by insufficient crater overlap (i.e., no topographic profiles intersected the overlapping area) or crater profiles exceeding the data extent near the poles, 404 (10.0%) are indeterminate, 177 and 223 (5.5%) yield conflicting relative ages. Many indeterminate pairs are associated with 178 179 large craters that have many craters impacting their rims (resulting in a highly variable rim 180 determination) that obscures rim topography in relation to the overlap area of any two crater pairs. On average, the older crater in an overlapping pair has a diameter of ~71 km, and the 181

younger has a diameter of ~35 km. 182

- 183
- 184 *3.2 Differences in Rim Elevation*
- 185 We measured the average and maximum rim elevation difference inside and outside the
- antecedent crater (Δz and $max(\Delta z)$, Fig. 1) for the 3,022 crater pairs for which we could
- 187 determine the relative age. We expect these rim elevation differences to scale with the size of the
- 188 antecedent relief, so we express elevation differences in terms of the antecedent crater depth (d).
- 189 Center-to-rim distance (δ , *Fig. 1*) informs whether the younger crater rim formed within the
- 190 antecedent crater floor, or closer to the antecedent rim and is also expected to influence the
- 191 observed rim elevation difference. Our results show that rim elevation differences are, on 192 average, close to zero where craters minimally overlap ($\delta > 0.8 R_o$) but decrease as center-to-rim
- distance decreases (Fig. 3). Average and maximum rim elevation differences decrease
- 194 approximately linearly until the young crater rim reaches the antecedent crater center ($\delta = 0 R_a$),
- 195 at which point the average and maximum rim elevation difference reach values of ~ -0.5 and -1 d, 196 respectively.
- 197

198 These observations demonstrate that crater rims are generally lower where they intersect the

antecedent negative topography of older craters and that the difference in rim elevation scales

with both the depth of the older crater and the degree of overlap of the two craters. In cases where the younger crater rim forms in the older crater center ($\delta \sim 0 R_o$), the lowest part of the

intersecting rim is $\sim 1 d$ lower than the exterior rim. However, this is not true for most crater pairs, in which the rim elevation difference is generally less than the antecedent crater depth.

- 204
- 205

206

207



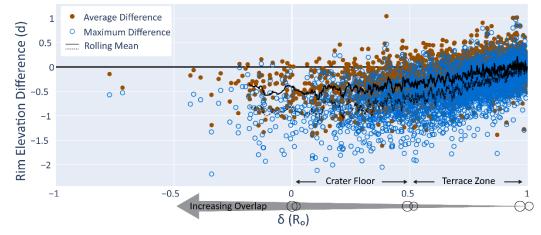


Fig. 3. Average and maximum rim elevation Difference vs. center-to-rim distance (δ) with rolling means for each group. Expected locations of the antecedent crater floor and terrace zone based

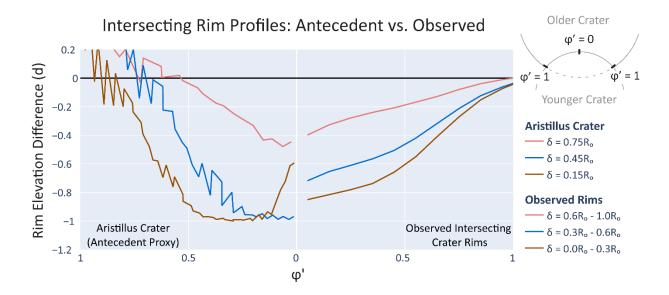
- 211 on scaling laws (Melosh, 1989, p. 198) and the average older crater diameter (71 km) are
- 212 marked. In crater pairs with $\delta < 0.5 R_o$, the young crater rim likely intersects the antecedent flat

- 214 *antecedent crater.*
- 215

²¹³ crater floor. Negative values of δ indicate that the younger crater covers the center of the

216 3.3 Intersecting Rim Shape and Topography

- 217 The prior results establish clear end cases: intersecting rims are not lower than exterior rims
- 218 when craters overlap minimally, and intersecting rims are lower by $\sim 1d$ when craters overlap
- substantially ($\delta \sim 0 R_o$). However, the gradual change in rim elevation difference (Fig. 3) does
- not reflect the shape of the antecedent craters which have a flat crater floor extending to $\sim 0.5 R_o$
- and a sharply rising terrace zone and rim (Melosh, 1989). This indicates that, in some crater pairs, the young crater rim formed within the antecedent crater floor (i.e., at -1 d) but is not 1 d
- lower than the exterior rim. To explore the causes of this apparent mismatch, we compare the
- topography along intersecting crater rims to several profiles of a pristine complex crater that
- serves as a proxy of antecedent crater topography (Fig. 4). We use Aristillus crater as our model
- 226 complex crater as it appears relatively pristine and has no intersecting craters within our crater
- size range.
- 228 The antecedent topography proxy (Fig. 4, left side) shows that as craters increase in overlap, the
- 229 young rim forms deeper into the antecedent basin, with the least overlapping craters (Fig. 4, $\delta =$
- 230 $0.75 R_o$) forming their rims fully within the terrace zone of the antecedent craters. In such cases,
- we would not expect to see a rim elevation difference equal to the depth of the antecedent crater,
- because the antecedent topography reaches only half the depth of the antecedent crater floor. However, for moderately and substantially overlapping crater pairs (Fig. 4, $\delta = 0.45, 0.15 R_o$),
- the antecedent topography clearly flattens and reaches depths of -1 d as it reaches the crater
- floor. For observed crater pairs at these high degrees of overlap (Fig 4, right side), no part of the
- crater rim reaches an elevation difference of -1 d, even at the deepest point of intersection. These
- 237 observed crater rim profiles also show little flattening at near $\varphi'=0$, though a mild slope break in
- the most deeply intersecting crater pairs (Fig 4, brown line) may reflect preservation of this
- antecedent feature. These comparisons reinforce a key finding from Fig. 3: that the rim elevation
- 240 difference of young crater rims forming in antecedent negative topography is generally less than
- -1 *d*. The topography of these intersecting crater rims also has less relief than the antecedent
- topography, but there is evidence that some elements of the antecedent topography (i.e., the slope
- 243 break corresponding to the terrace-to-floor transition) are preserved.



245

- 246 Fig. 4. (Right) Rim elevation difference for individual radial profiles vs. normalized azimuth (φ '
- 247 = $\varphi/(\theta_y/2)$). Data points are binned according to the absolute φ value. (Left) Smoothed
- 248 topography along a D = 35 km circle intersecting Aristillus Crater (D = 53 km) at various
- 249 distances: $\delta = 0.15$, 0.45, and 0.75 R_o . Line colors represent crater pairs with less overlap (δ
- 250 =0.6-1.0 R_o), moderate overlap (δ = 0.3-0.6 R_o), and substantial overlap (δ = 0.0-0.3 R_o).
- 251 *Craters with* $\delta < 0.45 R_o$ *are expected to intersect the flat crater floor, and the observed rim*
- topography is both elevated and smoothed relative to the expected antecedent topography.
- 253

254 3.4 Implications for Crater Formation Processes

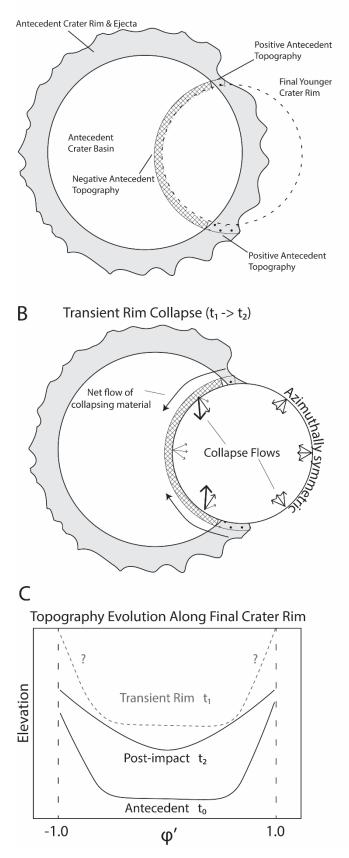
These observations show that crater rims are lower where they intersect older craters (Fig. 3), but 255 256 this lowering is not precisely predicted by the expected antecedent crater depth at the point of 257 rim formation. This mismatch between observed rim lowering and expected antecedent 258 topography provides insight into the way crater formation proceeds in the presence of antecedent 259 topography. To explain these observations, we infer that the younger crater's rim material must have been laterally or circumferentially distributed during crater formation, diffusing the effect 260 261 of the antecedent negative topography along the rim of the younger crater (Fig. 5). Some of this 262 diffusion may occur during the excavation and uplift stages of crater formation, but the collapse 263 of the transient rim is known to be critical in complex crater rim formation (Melosh and Ivanov, 1999; Senft and Stewart, 2009) and likely plays a larger role. A circumferential distribution of 264 265 rim materials during transient rim collapse of the younger crater readily explains the observations. First, crater rims are generally not lowered by the full depth of the antecedent 266 267 crater because circumferentially collapsing materials flow towards the deepest point of intersection. In the crater pairs with the greatest overlap ($\delta = 0 R_o$), we observe cases where the 268 269 maximum rim elevation difference reaches -1 d, demonstrating that there are limits to the extent 270 of this circumferential distribution of material. However, in most cases, this collapse is sufficient 271 to elevate the rim at the deepest point of intersection such that the maximum rim elevation difference is rarely -1 d. Second, the circumferential distribution of material during crater 272 273 formation would effectively smooth the initially sharp relief where the young crater rim 274 intersects the antecedent terrace and rim structures. This explains the observation of smooth, 275 elevated rims relative to the antecedent topography (Fig. 4), in which the floor-to-terrace

- 276 transition is no longer visible. This smoothing also explains why we see little evidence of
- 277 positive rim elevation differences where the young crater rim forms close to the antecedent crater
- rim or antecedent central peak, as these features are not laterally extensive enough to be
- 279 preserved in the young rim topography.

280 One caveat to these observations is the role of erosion – both erosion of the antecedent crater before the second impact and erosion of the younger crater after impact into the antecedent. To 281 282 first order, lunar erosion is well modeled by topographic diffusion (Craddock and Howard, 2000; 283 Fassett and Thomson, 2014), especially on a small scale. However, topographic diffusion may be limited by the slow breakdown of intact rock into regolith, and craters as small as 3 km do not 284 285 degrade as rapidly as would be predicted from diffusion (Fassett and Thomson, 2014). Erosion of 286 the antecedent crater before impact by the younger crater will not substantially change the key morphometric parameter: the depth of the crater relative to the surrounding terrain. Erosion of 287 288 the younger crater rim via diffusion would proceed much more rapidly in the radial direction 289 where the curvature is highest, relative to moderate changes in elevation along the crater rim. As

- such, the incredibly low yield strength of the collapsing transient crater provides a better explanation for the observed smooth rim profiles rather than post-impact diffusive erosion.

A Prior to Second Impact (t_o)



293 Fig. 5. Model of transient rim collapse asymmetries leading to the observed crater morphology.

(*A*) Shows the antecedent topography with indicators of where the new crater will form and the

antecedent topography relative to the surrounding terrain, (B) shows the moment of transient

rim collapse during the formation of the younger crater, and (C) illustrates the topographic

297 profile along the final crater rim location (Comparable to Figure 4). Asymmetries in the collapse

flow cause the rim to collapse towards the antecedent topography, smoothing the final rim

- 299 *profile relative to the antecedent topography.*
- 300

301 <u>4. Conclusions</u>

Using the Robbins crater database and a DEM of the lunar surface, we show that antecedent topography influences crater rim topography, and crater rims are systematically lower where they intersect antecedent craters. Additionally, these new crater rims only partially preserve the antecedent topography, and the difference in rim elevation inside and outside the new crater is not equal to the antecedent topographic relief in most cases. From these observations we suggest that transient rim collapse is an important process that may distribute material circumferentially

around the new crater rim, leading to the observed shape and relief.

309

310 These conclusions formalize and place constraints on the interaction of impact craters with

antecedent crater topography, a process that affects \sim 50% of complex craters on the moon (see

312 Method section) and many others in the solar system. The constraints we place on this

interaction, as well as the processes we propose to be responsible, have a bearing on the study of impact craters at large. Our results show that complex craters do not obliterate the underlying

315 topography and that crater rims bear signatures of the topography that preceded them. This

316 incomplete erasure of topography is an important consideration of crater saturation and crater

equilibrium(Hirabayashi et al., 2017), which depend sensitively on when craters are rendered

unobservable. Additionally, the asymmetric collapse process illustrated in Fig. 5 suggests that

the crater rim within the antecedent negative topography may have different geophysicalproperties compared to other portions of the crater rim. Impact simulations that include the

properties compared to other portions of the crater rim. Impact simulations that include the
 effects of dilatancy (Collins, 2014) suggest that collapsed transient rim materials have some of

the highest porosity of materials within the crater basin, notably higher than rim material. Crater

rims that form in antecedent topography may, therefore, be more porous than other sections of the crater rim, making them more prone to further modification, changing their gravitational

the crater rim, making them more prone to further modification, changing their gravitationalsignature, and potentially making them better reservoirs of subsurface fluids. Finally, several

Artemis landing sites are on the rims of complex craters with >1 km of height variability and one

site (Amundsen Crater Rim (NASA, 2022)) is a very clear case of a complex crater rim forming

within the basin of an older, complex, crater. This process of rim formation in overlapping crater

pairs is therefore an essential component of the geology of this site, and observations made *in*

330 *situ* by Artemis astronauts may further our understanding of how antecedent topography alters

- the crater formation process.
- 332
- 333 Acknowledgements

334 Dr. Don Hood was funded by the Baylor Office of the Vice Provost of Research Postdoctoral

- 335 Scholar program.
- 336

- 337 Data Availability Statement
- The data used in this work are available online via the USGS Astropedia Portal. The <u>Wide Angle</u>
- 339 Camera (WAC) mosaic, Global Lunar DTM (GLD) 100 Dataset, and Robbins Crater Database
- are all available for download. Data and code to generate the results we present is archived
- online via the Texas Data Repository as (Hood et al., 2024)
- 342 <u>https://doi.org/10.18738/T8/SYWIMY</u>.
- 343 344
- 345 Author Contributions:
- 346 **Don R. Hood:** Primary Authorship, Data Analysis, Methodological Development
- 347 Brennan W. Young: Data Analysis, Methodological Development, Manuscript Revisions
- 348 Aviv L. Cohen-Zada: Manuscript Revisions
- 349 Peter B. James: Manuscript Revisions, Science Oversight
- 350 Ryan C. Ewing: Manuscript Revisions, Science Oversight
- 351 Jeffery S. Lee: Manuscript Revisions, Science Oversight
- 352
- 353 <u>References</u>
- Aschauer, J., Kenkmann, T., 2017. Impact cratering on slopes. Icarus 290, 89–95.
 https://doi.org/10.1016/j.icarus.2017.02.021
- Bramson, A.M., Byrne, S., Putzig, N.E., Sutton, S., Plaut, J.J., Brothers, T.C., Holt, J.W., 2015.
 Widespread excess ice in Arcadia Planitia , Mars. Geophys. Res. Lett. 42, 1–9.
 https://doi.org/10.1002/2015GL064844
- Collins, G.S., 2014. Numerical simulations of impact crater formation with dilatancy. J.
 Geophys. Res. Planets 119, 2600–2619. https://doi.org/10.1002/2014JE004708
- 361 Craddock, R.A., Howard, A.D., 2000. Simulated degradation of lunar impact craters and a new
 362 method for age dating farside mare deposits. J. Geophys. Res. Planets 105, 20387–20401.
 363 https://doi.org/10.1029/1999JE001099
- Dundas, C.M., Mellon, M.T., Conway, S.J., Daubar, I.J., Williams, K.E., Ojha, L., Wray, J.J.,
 Bramson, A.M., Byrne, S., McEwen, A.S., Posiolova, L.V., Speth, G., Viola, D., Landis,
 M.E., Morgan, G.A., Pathare, A.V., 2021. Widespread Exposures of Extensive Clean
 Shallow Ice in the Midlatitudes of Mars. J. Geophys. Res. Planets 126.
 https://doi.org/10.1029/2020JE006617
- Elbeshausen, D., Wünnemann, K., Collins, G.S., 2009. Scaling of oblique impacts in frictional targets: Implications for crater size and formation mechanisms. Icarus 204, 716–731.
 https://doi.org/10.1016/j.icarus.2009.07.018
- Fassett, C.I., Thomson, B.J., 2014. Crater degradation on the lunar maria: Topographic diffusion
 and the rate of erosion on the Moon: Crater degradation on the lunar maria. J. Geophys.
 Res. Planets 119, 2255–2271. https://doi.org/10.1002/2014JE004698
- Grier, J.A., McEwen, A.S., Lucey, P.G., Milazzo, M., Strom, R.G., 2001. Optical maturity of
 ejecta from large rayed lunar craters. J. Geophys. Res. Planets 106, 32847–32862.
 https://doi.org/10.1029/1999JE001160
- Hartmann, W.K., Neukum, G., 2001. Cratering chronology and the evolution of Mars, in:
 Chronology and Evolution of Mars. Springer, pp. 165–194.
- Hirabayashi, M., Minton, D.A., Fassett, C.I., 2017. An analytical model of crater count
 equilibrium. Icarus 289, 134–143. https://doi.org/10.1016/j.icarus.2016.12.032

- Hood, D.R., James, P.B., Lee, J., 2023. Compositional and Morphometric Exploration of Van De
 Graaff Crater on the Lunar Farside, in: Lunar And Planetary Science Conference 2023. p.
 1658.
- Hood, D.R., Young, B.W., Cohen-Zada, A.L., James, P.B., Ewing, R.C., Lee, J.S., 2024.
 Supporting Data for "The Effect of Antecedent Topography on Complex Crater
 Formation." https://doi.org/10.18738/T8/SYWIMY
- Izquierdo, K., Sori, M.M., Soderblom, J.M., Johnson, B.C., Wiggins, S.E., 2021. Lunar
 Megaregolith Structure Revealed by GRAIL Gravity Data. Geophys. Res. Lett. 48.
 https://doi.org/10.1029/2021GL095978
- Krohn, K., Jaumann, R., Elbeshausen, D., Kneissl, T., Schmedemann, N., Wagner, R., Voigt, J.,
 Otto, K., Matz, K.D., Preusker, F., Roatsch, T., Stephan, K., Raymond, C.A., Russell,
 C.T., 2014. Asymmetric craters on Vesta: Impact on sloping surfaces. Planet. Space Sci.
 103, 36–56. https://doi.org/10.1016/j.pss.2014.04.011
- McEwen, A.S., Bierhaus, E.B., 2006. The Importance of Secondary Cratering to Age Constraints
 on Planetary Surfaces. Annu. Rev. Earth Planet. Sci. 34, 535–567.
 https://doi.org/10.1146/annurev.earth.34.031405.125018
- 398 Melosh, H.J., 1989. Impact Cratering: A Geologic Process. Oxford University Press, New York.
- Melosh, H.J., Ivanov, B.A., 1999. Impact crater collapse. Annu. Rev. Earth Planet. Sci. 27, 385–
 400 415. https://doi.org/10.1146/annurev.earth.27.1.385
- 401 NASA, 2022. NASA Identified Candidate Regions for Landing Next Americans on Moon.
- 402 Neish, C.D., Herrick, R.R., Zanetti, M., Smith, D., 2017. The role of pre-impact topography in 403 impact melt emplacement on terrestrial planets. Icarus 297, 240–251.
 404 https://doi.org/10.1016/j.icarus.2017.07.004
- 405 Neish, C.D., Madden, J., Carter, L.M., Hawke, B.R., Giguere, T., Bray, V.J., Osinski, G.R.,
 406 Cahill, J.T.S., 2014. Global distribution of lunar impact melt flows. Icarus 239, 105–117.
 407 https://doi.org/10.1016/j.icarus.2014.05.049
- Parker, M.V.K., Zegers, T., Kneissl, T., Ivanov, B., Foing, B., Neukum, G., 2010. 3D structure
 of the Gusev Crater region. Earth Planet. Sci. Lett. 294, 411–423.
 https://doi.org/10.1016/j.epsl.2010.01.013
- Pike, R.J., 1977. Size-dependence in the shape of fresh impact craters on the Moon, in: Impact and Explosion Cratering: Planetary and Terrestrial Implications. pp. 489–509.
- Riedel, C., Minton, D.A., Michael, G., Orgel, C., Bogert, C.H., Hiesinger, H., 2020. Degradation
 of Small Simple and Large Complex Lunar Craters: Not a Simple Scale Dependence. J.
 Geophys. Res. Planets 125. https://doi.org/10.1029/2019JE006273
- 416 Robbins, S.J., 2019. A New Global Database of Lunar Impact Craters >1-2 km: 1. Crater
 417 Locations and Sizes, Comparisons With Published Databases, and Global Analysis. J.
 418 Geophys. Res. Planets 124, 871–892. https://doi.org/10.1029/2018JE005592
- Scholten, F., Oberst, J., Matz, K.-D., Roatsch, T., Wählisch, M., Speyerer, E.J., Robinson, M.S.,
 2012. GLD100: The near-global lunar 100 m raster DTM from LROC WAC stereo image
 data: THE 100 M RASTER DTM GLD100. J. Geophys. Res. Planets 117, n/a-n/a.
 https://doi.org/10.1029/2011JE003926
- 423 Schwenzer, S.P., Abramov, O., Allen, C.C., Bridges, J.C., Clifford, S.M., Filiberto, J., Kring,
- 424 D.A., Lasue, J., McGovern, P.J., Newsom, H.E., Treiman, A.H., Vaniman, D.T., Wiens,
- 425 R.C., Wittmann, A., 2012. Gale Crater: Formation and post-impact hydrous
- 426 environments. Planet. Space Sci. 70, 84–95. https://doi.org/10.1016/j.pss.2012.05.014

- 427 Senft, L.E., Stewart, S.T., 2009. Dynamic fault weakening and the formation of large impact
 428 craters. Earth Planet. Sci. Lett. 287, 471–482. https://doi.org/10.1016/j.epsl.2009.08.033
- 429 Speyerer, E.J., Robinson, M.S., Denevi, B.W., the LROC Science Team, 2011. Lunar
 430 Reconnaissance Orbiter Camera Global Morphological Map of the Moon. Lunar Planet
 431 Sci Conf 2387.
- Wang, Y., Wu, B., Xue, H., Li, X., Ma, J., 2021. An Improved Global Catalog of Lunar Impact
 Craters (≥1 km) With 3D Morphometric Information and Updates on Global Crater
- 434 Analysis. J. Geophys. Res. Planets 126, e2020JE006728.
- 435 https://doi.org/10.1029/2020JE006728
- Wünnemann, K., Ivanov, B.A., 2003. Numerical modelling of the impact crater depth-diameter
 dependence in an acoustically fluidized target. Planet. Space Sci. 51, 831–845.
- 438 https://doi.org/10.1016/j.pss.2003.08.001
- 439